Discrete maximum entropy process modeling of uncertain properties: application to friction for stick-slip and microslip response

B.-K. Choi, M. C. Sipperley, M. P. Mignolet, Christian Soize

Discrete maximum entropy process modeling of uncertain properties: application to friction for stick-slip and microslip response

Byeong-Keun Choi [1,2], Mark C. Sipperley [1], Marc P. Mignolet [1], Christian Soize [3]

[1]SEMTE, Faculties of Mechanical and Aerospace Engineering, Arizona State University, Tempe AZ 85287-6106, USA
[2]Gyeongsang National University, Department of Energy and Mechanical Engineering, Tongyoung, Gyeongnam 650-160 Korea
[3]Université Paris-Est, LaboratoireModélisation et Simulation Multi-Echelle, MSME UMR 8208 CNRS, 5 Bd Descartes, 77454 Marne-la-Vallée, France
email: bgchoi@asu.edu, mark.sipperley@asu.edu, marc.mignolet@asu.edu, christian.soize@univ-paris-est.fr

ABSTRACT: The first part of the present investigation focuses on the formulation of a novel stochastic model of uncertain properties of media homogenous in the mean which are represented as stationary processes. In keeping with standard spatial discretization methods (e.g. finite elements), the process is discrete. It is further required to exhibit a specified mean, standard deviation, and a global measure of correlation, i.e. correlation length. The specification of the random process is completed by imposing that it yields a maximum of the entropy. If no constraint on the sign of the process exists, the maximum entropy is achieved for a Gaussian process the autocorrelation of which is constructed. The case of a process with constant sign is considered next and an algorithm is formulated to simulate the non-Gaussian process yielding the maximum entropy. In the second part of the paper, this non-Gaussian model is used to represent the uncertain friction coefficient in a simple, lumped mass model of an elastic structure resting on a frictional support. The dynamic response of this uncertain system to a random excitation at its end is studied, focusing in particular on the occurrence of slip and stick.

KEY WORDS: Uncertain properties, random process, uncertain friction, microslip, stick-slip

1 INTRODUCTION

The dramatic growth in computational capabilities over the last 20 years coupled with the continued development and refinement of finite element capabilities permits now the prediction of the dynamic response of very complex structures not only in their linear regime but also in the presence of local and global nonlinearities, either geometric (large deflections) or material. In fact, it could be argued that the accuracy with which the response can now be predicted is in general better or much better than the accuracy with which the system characteristics (geometry and material behavior) are known. This observation has led to a recently growing interest in incorporating geometry/material uncertainty in structural dynamic predictions.

This effort has often in the past been accomplished by modeling the uncertain properties as random variables, stochastic processes, or random fields (e.g. see [1-3]). In many practical situations, a key challenge in using such models to represent uncertain material or geometrical properties is the significant lack of information available on the uncertainty. The mean value of the property is often believed to be known from past experience and/or available data (e.g. Young's modulus of a particular material). The level (for example standard deviation) of uncertainty is often less clearly known and may in fact be considered as a variable in a parametric study. Sometimes, an upper and/or lower bound may also be known because of an acceptance/rejection test carried out on all samples. However, more detailed information is very often not available.

This perspective has led [4,5] to propose that the stochastic description of the uncertainty model be *derived* not assumed and further that it be derived by *maximizing the statistical entropy* under constraints representing the true knowledge on the stochastic model. The maximization of the entropy

induces a maximum spread of the uncertainty (consistently with the constraints) in the tail of the distribution and thus to the consideration of "wide-spread" uncertainty that provides a good perspective on the effects of variations of the system properties, even those that are "far" from the mean. Thus, this approach, which is referred to as the nonparametric stochastic modeling approach, requires only partial knowledge of the system uncertainty complemented by the single assumption of maximization of entropy.

In its original formulation [4,5], the nonparametric stochastic modeling approach was used for characterization of the mass, damping, and stiffness matrices of reduced order/modal models, not to the detailed characterization of any specific property (mass density, Young's modulus, etc.). Thus, the resulting formulation is able to globally model all of them, as well as geometric uncertainties. More recently, this approach has been extended to matrix-valued fields, in particular for the modeling for the elasticity tensor of random media [6]. The present effort complement this work by addressing the modeling of random properties, of variable or constant sign, of media homogenous in the mean as stationary processes. In keeping with standard spatial discretization methods (e.g. finite elements), the process is discrete. The methodology relies on the specification of only the mean and standard deviation of the property as well as on a global measure of the correlation, i.e. a correlation length. The maximization of the entropy then provides the description of the process consistent with this prescribed information.

In regards to application, it is desired here to exemplify this modeling strategy on a property seldom considered and yet exhibiting well known uncertainty, i.e. friction. When two deformable bodies are in extended contact with each other, as in joints, turbomachinery blade friction dampers, brakes, etc., the coefficient of friction between them must be defined over

the contact zone, i.e. as a spatially varying property which governs the occurrence of stick, microslip, or macroslip [7-11]. After an appropriate spatial discretization of the contact zone, it becomes then necessary to specify the coefficient of friction at a set of discrete locations. The uncertainty in the values of this coefficients resulting from unknown spatial variations of roughness, temperature, composition, etc. then calls for the stochastic modeling considered in the first part of the paper. To demonstrate this application and presents a first perspective in this problem, a simple dynamic model of this contact problem is adopted here as a cascade of 5 Iwan oscillators. The response of this system to a white noise excitation at one end, the other one being fixed, is numerically determined and the effects of the uncertainty level (standard deviation) and correlation length are assessed.

2 MAXIMUM ENTROPY DISCRETE PROCESS

2.1 General derivation

Let X_n denote a discrete stationary process defined over the domain $n \in I = \{l, l+1, \ldots, u\}$ and define the random vector $\underline{X} = [X_l \, X_{l+1} \ldots X_u]^T$ where T denotes the operation of matrix/vector transposition. Then, the entropy S is a statistic of $\underline{X}$ that measures its dispersion/variability in a manner different from the variance. It is defined as

$$S \equiv -E\left[\ln\left(p_{\underline{X}}(\underline{X})\right)\right] = -\int_\Omega \ln\left(p_{\underline{X}}(\underline{x})\right) p_{\underline{X}}(\underline{x}) d\underline{x} \qquad (1)$$

where $E[.]$ denotes the operation of mathematical expectation and Ω is the domain of support of the values of the process. If no signature constraint is enforced, both positive and negative values of the process are allowed and thus

$$\Omega = \left\{(x_l, x_{l+1}, \ldots, x_u) \in (-\infty, \infty) \times (-\infty, \infty) \ldots \times (-\infty, \infty)\right\}. \qquad (2)$$

If a positive sign of the process is required,

$$\Omega = \left\{(x_l, x_{l+1}, \ldots, x_u) \in [0, \infty) \times [0, \infty) \ldots \times [0, \infty)\right\}. \qquad (3)$$

In Eq. (1), $p_{\underline{X}}(\underline{x})$ denotes the probability density function of the random vector $\underline{X}$ evaluated at a possible realization point $\underline{x}$. Since the process X_n underlying the random vector $\underline{X}$ is stationary, the joint probability density function $p_{\underline{X}}(\underline{x})$ must satisfy the usual independence under a uniform shift along I, e.g.

$$p_{X_n}(x) = p_{X_{n+1}}(x) \quad \text{and} \quad p_{X_n X_m}(x, y) = p_{X_{n+1} X_{m+1}}(x, y). \qquad (4)$$

It is desired here to determine $p_{\underline{X}}(\underline{x})$ that maximizes the entropy, Eq. (1), under the constraints that
(1) that the total probability is one, i.e.

$$\int_\Omega p_{\underline{X}}(\underline{x}) d\underline{x} = 1 \qquad (5)$$

(2) that the mean value is given and constant (since the process is stationary)

$$E[X_n] = \int_\Omega x_n \, p_{\underline{X}}(\underline{x}) d\underline{x} = \mu_X \qquad n \in I \qquad (6)$$

(3) that the variance is given and constant (again, relying on the stationary of the process)

$$E\left[(X_n - \mu_X)^2\right] = \int_\Omega (x_n - \mu_X)^2 \, p_{\underline{X}}(\underline{x}) d\underline{x} = \sigma_X^2 \qquad n \in I \qquad (7)$$

(4) and that a given measure of the correlation, i.e. a correlation length is given. Two such measures that have been introduced in the past are

$$L_0 = \frac{\sum_{m=1}^{\infty} |K_{XX}(m)|}{K_{XX}(0)} \quad \text{and} \quad L_1 = \frac{\sum_{m=0}^{\infty} m |K_{XX}(m)|}{\sum_{m=0}^{\infty} |K_{XX}(m)|} \qquad (8),(9)$$

where

$$K_{XX}(m) = \Gamma_{XX}(n, n+m) = E\left[(X_n - \mu_X)(X_{n+m} - \mu_X)\right]$$
$$= \int_\Omega (x_n - \mu_X)(x_{n+m} - \mu_X) p_{\underline{X}}(\underline{x}) d\underline{x} \quad \text{for any } n \in I \qquad (10)$$

is the stationary autocovariance function. Numerically, the series involved in Eqs (8) and (9) will be approximate by finite sum for $m = 0$ to $m_{\max}$. Then, Eqs (8) and (9) can both be written as

$$\sum_{m=0}^{m_{\max}} a_m s_m K_{XX}(m) = 0 \quad \text{or as} \quad \sum_{m=0}^{m_{\max}} a_m s_{m,n} \Gamma_{XX}(n, n+m) = 0$$
$$\text{for any } n \qquad (11a),(11b)$$

where

$$s_m = \text{sgn}(K_{XX}(m)) \qquad s_{m,n} = \text{sgn}[\Gamma_{XX}(n, n+m)] \qquad (12a),(12b)$$

and for appropriate coefficients a_m. Specifically,

$$a_m = (1 + L_0) \delta_{m0} - 1 \qquad m \in [0, m_{\max}] \qquad (13)$$

for the correlation length L_0 while for L_1

$$a_m = L_1 - m \qquad m \in [0, m_{\max}] \qquad (14)$$

In the next section, it will be shown that the maximization of the entropy under the constraints of Eqs (5), (6), (7), and (11b) exhibits a generally undesirable behavior. To prevent this issue, the variance constraint of Eq. (7) will be replaced by the general scaling condition

$$K_{xx}(0) + U \sum_{m=1}^{\infty} K_{xx}(m) m^p = N \qquad (15)$$

or, in terms of $\Gamma_{XX}(n, m)$ and truncating the summation to $m = m_{\max}$

$$\Gamma_{XX}(n, n) + U \sum_{m=1}^{m_{\max}} \Gamma_{XX}(n, n+m) m^p = N \quad \text{for any } n \qquad (16)$$

where N is finite. Although the motivation for this condition is presented below, note here that for $U = 0$, Eq. (16) reduces exactly to Eq. (7) of which it can thus be recognized as a generalization.

For the optimization of the entropy, it is convenient to rewrite Eqs (5), (6), (11b), and (16) in the generic form

$$\Xi_{in} \equiv \int_\Omega f_{in}(\underline{x}) p_{\underline{X}}(\underline{x}) d\underline{x} - C_i = 0 \qquad (17)$$

where

$$f_{1n}(x_n) = x_n - \mu_X \quad \text{and} \quad C_1 = 0 \qquad (18a), (18b)$$

$$f_{2n}(\underline{x}) = \sum_{m=0}^{m_{\max}} a_m s_m (x_n - \mu_X)(x_{n+m} - \mu_X) \quad C_2 = 0 \quad (19a), (19b)$$

$$f_{3n}(\underline{x}) = \sum_{m=1}^{m_{max}} U\,m^p\,(x_n - \mu_X)(x_{n+m} - \mu_X) + (x_n - \mu_X)^2$$

$$C_3 = N \qquad (20a),\,(20b)$$

and finally $\qquad f_4 = 1 \qquad$ and $\qquad C_4 = 1$. $\qquad$ (21a), (21b)

Then, the maximization of the entropy, Eq. (1) under the constraints of Eqs (17)-(21) can be accomplished in the Lagrange multiplier framework through the unconstrained maximization of

$$S^* = S - \sum_n \lambda_{1n}\,\Xi_{1n} - \sum_n \lambda_{2n}\,\Xi_{2n} - \sum_n \lambda_{3n}\,\Xi_{3n} - \lambda_4\,\Xi_4 \quad (22)$$

where λ_{1n}, λ_{2n}, λ_{3n}, and λ_4 are the Lagrange multipliers associated with the above constraints. This process leads to the probability density function

$$p_{\underline{X}}(\underline{x}) = \frac{1}{e} \exp\left[-\sum_n \lambda_{1n} f_{1n} - \sum_n \lambda_{2n} f_{2n} - \sum_n \lambda_{3n} f_{3n} - \lambda_4 f_4 \right]$$
$$\underline{x} \in \Omega. \qquad (23)$$

Next, note that the term in bracket is a quadratic form of the vector $\underline{x} - \mu_X \underline{E}$, where $\underline{E}$ is the vector whose components are all equal to 1, i.e. $\underline{E} = [\ldots 111\ldots]^T$. Thus, Eq. (23) can be rewritten as

$$p_{\underline{X}}(\underline{x}) = C' \exp\left[-\frac{1}{2}(\underline{x} - \mu_X\underline{E})^T G'(\underline{x} - \mu_X\underline{E}) - \underline{V}^T(\underline{x} - \mu_X\underline{E}) \right]$$
$$\underline{x} \in \Omega \qquad (24)$$

where $\qquad C' = \exp(-\lambda_4 - 1) \qquad$ (25)

$$G'_{n(n+m)} = 2\,\lambda_{2n}\,[a_m\,s_m] + 2\,\lambda_{3n}\,[U\,m^p + \delta_{m0}] \quad m \in [0, m_{max}]$$
$$(26)$$

0 otherwise, and

$$V_n = \lambda_{1n}. \qquad (27)$$

Note in Eq. (26) that δ_{ij} denotes the Kronecker symbol. Assuming that the matrix G is not singular, Eq. (24) can finally be rewritten as

$$p_{\underline{X}}(\underline{x}) = C \exp\left[-\frac{1}{2}(\underline{x} - \underline{\mu})^T G(\underline{x} - \underline{\mu}) \right] \quad \underline{x} \in \Omega \qquad (28)$$

where $\qquad C = C' \exp\left[\frac{1}{2}\underline{V}^T G^{-1} \underline{V} \right] \qquad$ (29)

$$\underline{\mu} = \mu_X\,\underline{E} - G^{-1}\underline{V} \qquad (30)$$

$$G = \frac{1}{2}\left(G' + G'^T\right). \qquad (31)$$

To complete the characterization of the distribution of Eq. (28), it remains to evaluate the parameters it involves, i.e. the Lagrange multipliers λ_{1n}, λ_{2n}, λ_{3n}, and λ_4, from the constraints they represent, i.e. Eqs (5), (6), (11b), and (16). In that regard, note that it is more convenient to directly focus on the evaluation of C, $\underline{\mu}$, λ_{2n}, and λ_{3n} the latter two defining the matrices G' and G.

Of special interest here is the situation where the size of the domain I becomes large, i.e. $l \to -\infty$ and $u \to \infty$. In this case, each random variable X_n exhibits the same properties,

none of them being closer or further from the boundaries l and u of the domain I and thus the dependence of $p_{\underline{X}}(\underline{x})$ on any variable x_n should be the same. This condition is matched when

$$\underline{\mu} = \mu\underline{E}, \quad \lambda_{2n} = \lambda_2 \quad \text{and} \quad \lambda_{3n} = \lambda_3 \quad (32a),(32b),(32c)$$

in which case the matrix G is Toeplitz and symmetric. With Eqs (32b) and (32c), the matrix G' becomes

$$G'_{n(n+m)} = (2\,\lambda_3)\left\{ \delta_{m0} + U\,m^p + \delta\,a_m s_m \right\} \quad m \in [0, m_{max}] \quad (33)$$

where the parameter $\delta = \lambda_2/\lambda_3$ is introduced in place of λ_2. Note here that the signs $s_m = \pm 1$ are dependent on the autocorrelation function, see Eq. (12a), and thus are unknown at this point. This issue will be addressed in the ensuing sections.

Equations (28), (31), (32a), and (33) represent the maximum entropy distribution sought. To be useful in practical situations, it remains to address the following three issues:

(1) the determination of the parameters C, μ, λ_3, s_m, and δ from Eqs (5), (6), (7), and (11a) (at this stage, the normalization condition of Eq. (7) is reinstated in place of Eq. (16), although the parameters U and p continue to appear in Eq. (33)) and the efficient simulation of realization of the random values X_n when

$$\Omega = \{(x_l, x_{l+1}, \ldots, x_u) \in (-\infty, \infty) \times (-\infty, \infty) \ldots \times (-\infty, \infty)\}.$$

(2) the selection of the parameters U and p following a discussion of the need to introduce Eq. (16).

(3) the determination of the parameters C, μ, λ_3, s_m, and δ from Eqs (5), (6), (7), and (11a) and the efficient simulation of realization of the random values X_n when

$$\Omega = \{(x_l, x_{l+1}, \ldots, x_u) \in [0, \infty) \times [0, \infty) \ldots \times [0, \infty)\}.$$

These 3 issues are addressed in the ensuing sections.

2.2 Process without sign constraint

The case of a process without sign constraint, i.e. with the domain Ω defined by Eq. (2) is considered first because of its simplicity. Under this assumption, it is concluded from Eq. (28) that the random vector $\underline{X}$ is Gaussian with mean $\underline{\mu}$ and with covariance matrix

$$\hat{K}_{XX} = G^{-1}. \qquad (34)$$

Note that $\hat{K}_{XX}$ is expected to exhibit a Toeplitz structure, as G does, owing to the stationarity of the process in its autocorrelation function.

To satisfy the constraints of Eqs (5) and (6), one obtains directly

$$C = \sqrt{\frac{\det(G)}{(2\pi)^P}} \qquad (35)$$

where P denotes the number of values of the process considered and

$$\mu = \mu_X. \qquad (36)$$

Next, consider the parameter λ_3 and note that it scales (for a fixed value of δ) the matrices G and $\hat{K}_{XX}$. In fact, the latter

is inversely proportional to it demonstrating that the effect of λ_3 is to uniformly scale the values of the process by the factor $1/\sqrt{|\lambda_3|}$ and to modify the sign of the autocovariance function. Thus, this parameter does not affect the correlation length which is a ratio of autocorrelation values and accordingly is only a function of δ and the selected sign sequence s_m (see Eq. (12a)). Once these quantities have been determined from either Eq. (8) or (9) and Eq. (12a), i.e. by solving

$$L_0(\delta, s_m) = \overline{L}_0 \quad \text{or} \quad L_1(\delta, s_m) = \overline{L}_1 \tag{37}$$

where $\overline{L}_0$ or $\overline{L}_1$ is the imposed correlation length, the value of λ_3 can then be selected to match the variance condition, Eq. (7).

The numerical evaluation of $L_0(\delta, s_m)$ and $L_1(\delta, s_m)$ for specified values of $m_{\max}$, U and p, and for a given value of δ and of the sign sequence s_m was achieved as follows. The matrix G/λ_3 was first formed for $P = 2*M +1$ random variables X_n. The parameter M was selected "large enough", i.e. much larger than $m_{\max}$ for the inverse $(G/\lambda_2)^{-1} = \widetilde{K}_{\underline{X}\underline{X}}$ to exhibit a near Toeplitz structure. Since the convergence to this structure occurred faster for the elements near the center of the matrix, the $M + 1$st row was considered representative of the true infinite Toeplitz matrix and was used for the estimation of the autocorrelation values as

$$K_{XX}(m) = \frac{1}{\lambda_3} \left(\widetilde{K}_{\underline{X}\underline{X}} \right)_{M+1, M+1+m}. \tag{38}$$

Since the variance $K_{XX}(0)$ must be positive, the sign of λ_3 was determined to enforce that condition on the autocorrelation sequence of Eq. (38), i.e. $\text{sgn}(\lambda_3) = \text{sgn}\left[\left(\widetilde{K}_{\underline{X}\underline{X}} \right)_{M+1, M+1} \right]$. Then, the correlation length, $L_0(\delta, s_m)$ or $L_1(\delta, s_m)$, and the sign $\text{sgn}(K_{XX}(m))$ were estimated and compared to $\overline{L}_0$ or $\overline{L}_1$ and s_m. A matched of both indicated that an acceptable solution of the values δ and s_m was found. Next, the magnitude of λ_3, was determined to satisfy the variance normalization condition, Eq. (7). Finally, the constants μ and C were obtained from Eqs (35) and (36) completing the determination of the probability density function.

Multiple solutions (acceptable values δ and s_m) were occasionally found. In such cases, the solution yielding the lowest value of the entropy was retained. In this regard, introducing the expression of the probability density function given by Eq. (28) in Eq. (1) yields

$$S = -\ln C + \frac{1}{2} E \left[\left(\underline{X} - \underline{\mu} \right)^T G \left(\underline{X} - \underline{\mu} \right) \right] \tag{39}$$

or, using Eq. (36),

$$S = -\ln C + \frac{P}{2}. \tag{40}$$

The simulation of random values X_n can be achieved by standard algorithms. In particular, samples of the random

vector $\underline{X}$ can be obtained from the relation

$$\underline{X} = \underline{\mu} + L\underline{W} \tag{41}$$

where L is the Cholesky decomposition of G^{-1}, i.e. $G^{-1} = LL^T$, and the components of the vector $\underline{W}$ are independent zero mean and unit variance Gaussian random variables.

2.3   Normalization condition: Eq. (16) vs. Eq. (7)

The discussion carried out in the previous section is applicable for any values of U and p of the constraint of Eq. (16) and thus are also valid for $U = 0$, i.e. when the variance constraint of Eq. (7) is directly imposed. This special case was considered here first for the 2 definitions of the correlation length, Eqs (8) and (9), for $\overline{L}_0$ or $\overline{L}_1$ =0.3, and for several values of $m_{\max}$, e.g. see Fig 1.
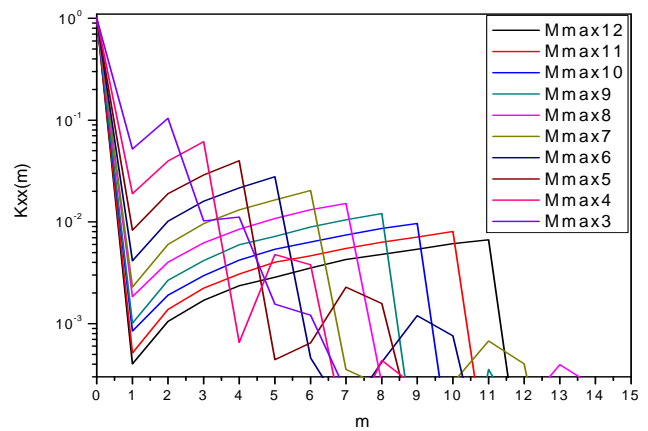

Figure 1. Autocovariance functions obtained for $U = 0$, $\sigma_X = 1$, $\overline{L}_1$ =0.3, and various $m_{\max}$.

An inspection of this figure (note the logarithmic scale) indicates that the autocorrelation function values for lags $m \geq 1$ are steadily decreasing values, e.g. the peak value away from zero is monotonically decreasing. Extrapolating this behavior to $m_{\max} \to \infty$ suggests that the autocovariance values will converge to near zero values, i.e. that the process will converge to a white noise, which is the solution of the problem in the absence of the correlation length constraint. Further, this latter condition is satisfied by the autocovariance function exhibiting a near constant value (for the L_0 definition, not shown here fro brevity) or a growing behavior in $m \in [1, m_{\max}]$ (for the L_1 definition).

This behavior is clearly not the one which is desired. The truncation of the summations in Eqs (8) and (9) to $m_{\max}$ was motivated by computational requirements and should have little effect for $m_{\max}$ large enough at the contrary of the trend shown in Fig 1. The desired behavior is achieved here through the U dependent term in Eq. (15) which, with $p > 0$ for the L_0 definition and 1 for the L_1 definition, weighs more heavily the terms of the autocovariance function near $m = m_{\max}$ than the correlation length constraint and thus forces this function to converge faster. Note however that two new parameters, U

and p, appear in this process and their rational selection must be formulated.

If the desired convergence of the autocovariance function is achieved, the truncation of the summations in Eq. (8) or (9) should have a small effect on the value of the correlation length. This effect can be measured by the error

$$\varepsilon_{trunc} = \frac{\sum_{m=1}^{M}|K_{XX}(m)| - \sum_{m=1}^{m_{max}}|K_{XX}(m)|}{K_{XX}(0)} \qquad \text{or}$$

$$\varepsilon_{trunc} = \frac{\sum_{m=0}^{M}m|K_{XX}(m)|}{\sum_{m=0}^{M}|K_{XX}(m)|} - \frac{\sum_{m=0}^{m_{max}}m|K_{XX}(m)|}{\sum_{m=0}^{m_{max}}|K_{XX}(m)|} \qquad (42)$$

if the definitions L_0 or L_1 of the correlation length are used. Note in the above equations that M is the largest lag that can be estimated from the inversion of the matrix G. Then, the selection of the parameter U, for a given value of m_{max}, was achieved to yield the lowest value of the truncation error ε_{trunc}.

A similar strategy could be proposed for the determination of the best value of p but this process has been observed to lead to p converging to its minimum value allowed, i.e. 0 for the L_0 definition and 1 for the L_1 definition. Thus, a fixed value of p was imposed. Specifically, this parameter was chosen equal to 2 as Eq. (15) then leads to a physically-based condition. Indeed, recognizing that the power spectral density of the process $Y_n = X_n - \mu_X$ is defined as

$$S_{YY}(\omega) = \frac{1}{2\pi}\sum_{m=0}^{\infty}R_{YY}(m)\cos m\omega = \frac{1}{2\pi}\sum_{m=0}^{\infty}K_{XX}(m)\cos m\omega$$
$$(43)$$

and assuming that the convergence is uniform in ω, it is found that

$$\sum_{m=1}^{\infty}m^2 K_{XX}(m) = 2\pi\left[\frac{d^2 S_{YY}(\omega)}{d\omega^2}\right]_{\omega=0}. \qquad (44)$$

Thus, Eq. (15) is equivalent to the imposition of a nonzero value of the curvature of the spectrum $S_{YY}(\omega)$ at zero frequency

$$\left[\frac{d^2 S_{YY}(\omega)}{d\omega^2}\right]_{\omega=0} = \frac{1}{2\pi U}[N - K_{XX}(0)] \qquad (45)$$

thereby preventing the occurrence of a white noise solution characterized by $S_{YY}(\omega) = $ constant or $\left[\frac{d^2 S_{YY}(\omega)}{d\omega^2}\right]_{\omega=0} = 0$.

In summary, the determination of the parameters of the distribution of Eqs (28), (32), (33) and the simulation of random values of the process thus proceeded as follows. For fixed values of m_{max}, U, and the autocorrelation sign sequence s_m, the parameters δ and λ_3 were determined to yield the given correlation length value (based on m_{max} lags), i.e. Eqs (11a) and (37), and the variance constraint of Eq. (7). These computations were repeated by specifying in turn each

sign sequence s_m and the optimum cases in which this vector matched the sign sequence of the computed autocovariance function $K_{XX}(m)$ for $m \in [1, m_{max}]$ were identified. Of this set was retained the one leading to the largest entropy as evaluated from Eq. (40) and the corresponding truncation error, Eq. (42), was determined. This effort was repeated by varying U until a minimum of the truncation error was achieved. Finally, the above process was repeated for increasing values of m_{max} and stopped when either a decrease of entropy or an increase in truncation error of the final solution was obtained.
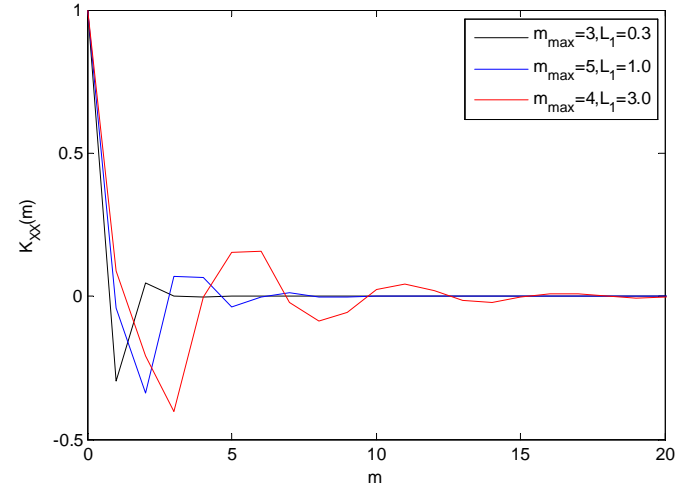

Figure 2. Autocovariance functions for correlation lengths of 0.3, 1, and 3 for the definitions of Eq. (9).

Shown in Fig. 2 are the autocovariance functions obtained with this approach for correlation length of 0.3, 1, and 3 and for the definitions of the correlation lengths of Eq. (9). Clearly, these autocovariance functions do exhibit the expected features and the appropriate convergence as the lag number is increased. Note further that the form of this function depends on the choice of the correlation length definition, the curves obtained with Eq. (8) do not appear to oscillate significantly while those obtained with Eq. (9) do. With these autocovariance functions, the simulation of random values X_n follows from Eq. (41).

2.4 Positive processes

Many physical properties are positive and thus the modeling of their uncertainty must maintain this constraint. In the present formulation, this is achieved by restricting the process to exhibit only positive values, i.e. with $\Omega = \{(x_l, x_{l+1},...,x_u) \in [0,\infty) \times [0,\infty)... \times [0,\infty)\}$. In this case, Eq. (28) is a truncated Gaussian distribution which *does not* vanish when any of the variable x_n goes to zero. This feature of the obtained distribution is not acceptable for certain properties which must be strictly positive and accordingly the work carried out in this section is unsuitable to model their uncertainties.

Assuming that strict positiveness is not required, it is next necessary to determine the parameters C, μ, λ_3, s_m, δ, and U to satisfy the stated constraints. In this regard, the key difference with the case in which the process has no sign

constraint is the lack of closed form expressions for the normalization constant, mean, and covariance matrix, i.e. Eqs (34)–(36) are no longer applicable as the random vector $\underline{X}$ is no longer jointly Gaussian, only truncated Gaussian. Accordingly, it will be necessary to simulate values of the process X_n first to impose the matching of the mean, Eq. (6), variance, Eq. (7), correlation length, Eq. (11), and sign sequence, Eq. (12), constraints.

The simulation of such values for specified values of μ, λ_3, s_m, δ, and U will be achieved by rejection from the jointly Gaussian vector $\underline{Y}$, or equivalently the Gaussian process Y_n, defined as in Eq. (28) but over the entire space, i.e.

$$p_Y\left(\underline{y}\right) = C\exp\left[-\frac{1}{2}\left(\underline{y}-\underline{\mu}\right)^T G\left(\underline{y}-\underline{\mu}\right)\right]$$
$$\underline{y} \in \left(-\infty,\infty\right)\times\left(-\infty,\infty\right)\ldots\times\left(-\infty,\infty\right). \qquad (46)$$

While this vector could be simulated according to the strategy of Eq. (41), this would lead to an expensive rejection process as any simulated vector $\underline{y}$ with at least one negative value would be discarded. A better approach is to proceed *sequentially* and to simulate values y_n, $n=1, 2, \ldots$ (achieved here using an autoregressive modeling approach) from which the corresponding values x_n are obtained. Specifically, $x_n = y_n$ if y_n is positive. If this simulated value is negative, another y_n is simulated and checked for positiveness. This simulation is repeated at step n until a positive value y_n is obtained and the assignment $x_n = y_n$ carried out. The simulation then moves to step $n+1$ and is repeated until the number of samples generated is large enough to conduct a statistical analysis giving the stationary mean and autocovariance function of the process X_n. These values are then used to evaluate the closeness to the mean, Eq. (6), variance, Eq. (7), correlation length, Eq. (11), and sign sequence, Eq. (12), conditions. These computations are iterated for given values of m_{max} and U, to obtain the parameters μ, λ_3, s_m, and δ. As in the case of processes without sign constraints, an outer loop is carried out to determine the optimum value of U to minimize the truncation error and further performed for increasing m_{max} as long as the entropy increases and the truncation error decreases.

As in the case of processes without sign constraint, multiple set of values μ, λ_3, s_m, and δ were occasionally found to satisfy the mean, variance, correlation length, and autocovariance sign sequence constraints. In such cases, the solution which was retained was the one yielding the largest value of the entropy. This quantity was determined here as in Eq. (39). However, since μ is no longer the mean value μ_X, one obtains

$$S = -\ln C + \frac{P}{2} + \left[\underline{\mu}_X - \underline{\mu}\right]^T G\left[\underline{\mu}_X - \underline{\mu}\right] \qquad (47)$$

where the constant is expressed as

$$C = \sqrt{\frac{\det(G)}{(2\pi)^P}}\frac{1}{\left(1-p_{rej}\right)} \qquad (48)$$

where p_{rej} is the probability of rejection of samples according to the simultaneous simulation algorithm of Eq. (41), i.e. $1-p_{rej} = \mathrm{Prob}\left[\underline{Y}\in\mathrm{R}^P\right]$. In the autoregressive-based algorithm, this probability can also be evaluated using conditional probabilities. Specifically,

$$1-p_{rej} = \prod_{s=1}^{P}\mathrm{Prob}\left[Y_s\in\mathrm{R}\mid\underline{Y}_{s-1}\in\mathrm{R}^{s-1}\right] = \prod_{s=1}^{P}\left(1-p_{rej}^{(s)}\right)$$
$$(49)$$

where $\underline{Y}_s$ denotes the vector with the components Y_n with $n = 1, \ldots, s$ and $p_{rej}^{(s)}$ is the probability of rejecting the sample s having accepted the previous one.

The above process was exemplified with the correlation length definition of Eq. (8) and with $\overline{L}_0 = 3$ with means of 1, 2, and 3. With the variance fixed at 1, these values of the mean led to coefficients of variations equal to 1/3, 1/2, and 1. For comparison, the values of m_{max} were kept equal to the optimum values found in the case of a process without sign constraint. The resulting autocovariance functions of the positive processes are shown in Fig. 3. Also shown on these figures are the autocovariance function in the non positive (no sign constraint) case. As expected, these latter values closely match their counterpart for the mean of 3 (coefficient of variation of 1/3) but in fact, it is found that the autocovariance function is almost independent of the mean/coefficient of variation even at the highest level of variation used.
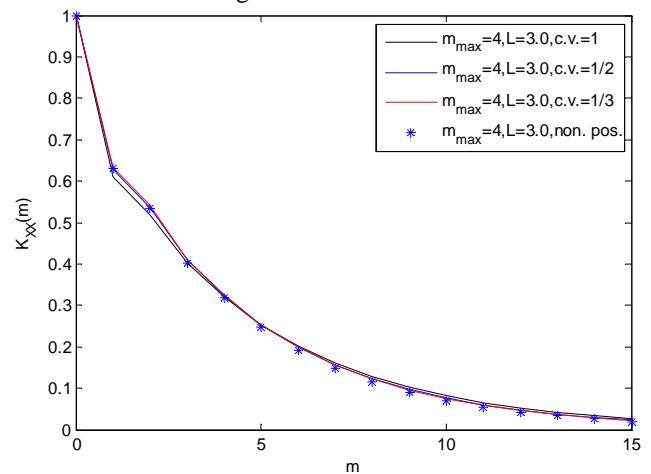

Figure 3. Autocovariance functions of the optimal positive process for correlation lengths of 3 for the definitions of Eq. (8) and for coefficients of variation ("c.v.") of 1/3, 1/2, and 1.

3   APPLICATION TO FRICTION MODELING IN STICK-SLIP AND MICROSLIP RESPONSE

One objective of the present study was to investigate the effects of uncertainty in the friction coefficients on the dynamic response of systems exhibiting stick-slip and microslip behavior and the methodology developed in the previous sections provides the modeling of the uncertain friction coefficients. To demonstrate its application, consider the 5-degree-of-freedom system shown in Fig. 4 consisting of a chain of Iwan oscillators. Each of the degrees-of-freedom in this system are connected to ground through a slider/friction

element which slides when the force in the corresponding spring is larger than the force of friction.
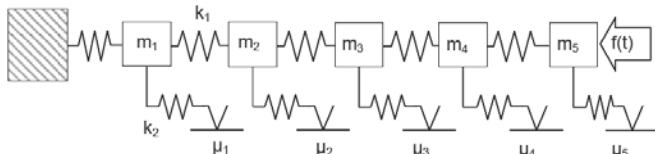

Figure 4. Chain of Iwan oscillators considered.

The parameters of the each oscillator were selected to be identical, i.e. the masses were chosen as $m_i = m = 1$ kg while the stiffnesses k_1 and k_2 were selected as 25N/m and 50N/m, respectively. In regards to the friction, the value of the normal force N was assumed to equal 10 and the static and kinematic coefficients of friction were taken equal, i.e. $\mu_S^{(i)} = \mu_D^{(i)}$ for each oscillator i =1, ..., 5. Further, the mean model of the system was assumed to have coefficients of friction $\mu_S^{(i)} = \mu_D^{(i)} = 0.2$ for each oscillator i =1, ..., 5. In addition, the stuck system was assumed to also exhibit a classical viscous damping with a modal damping ratio of 0.5% on all 5 modes.

Note that the consideration of viscous damping in addition to friction is necessary as the latter does not guarantee alone the finiteness of the response (e.g. see discussion of [7]). However, the viscous damping is sufficient, i.e. even without friction, to ensure this finiteness condition. Thus, the strict positiveness of the simulated coefficients of friction is not required and accordingly, the uncertainty modeling approach described in the previous section is applicable.

The system was subjected to a concentrated force at its free end varying in time as a Gaussian white noise process in the range of [0,60] Hz with a specified variance (see below). The response of the system was obtained through a Newmark integration scheme with a standard time step of 8.4 10^{-3}s. Particular care was exercised to accurately pinpoint the transitions of the degrees-of-freedom from slip to stick and stick to slip. The transition capturing was accomplished by a successive halving of the time steps when a transition was detected until the step was 2^{15} time smaller than the standard time step. At that point, transition was assumed to be at the beginning or the end of this small interval depending on the closeness of the transition from these end points. The validation of the algorithm was accomplished by tracking various transitions.

For these parameter values, it was desired next to select a value of the excitation variance that would provide stick-slip of the various masses to exemplify microslip. For low values of the variance, the system remains stuck and the response is linear. As the variance of the excitation is increased, the system slowly changes from fully stuck to fully slipping and the frequencies at which the peak of the response power spectra slowly reduce transitioning from the natural frequencies of the stuck system (1.15, 1.31, 1.53, 1.75, and 1.90Hz) to their counterparts from the slipping one (0.23, 0.66, 1.04, 1.34, and 1.53Hz). For intermediate values of the variance, e.g. 3.7 N^2, the desired stick-slip behavior is achieved but differently for each oscillator. Specifically, the fraction of time spent in slip mode decreases monotonically

from the degree-of-freedom 5 on which the force is applied to the first one, nearest to the wall: 37%, 22%, 12%, 8%, and 7%, respectively.

Uncertainty in the coefficients of friction was introduced with the positive definite process with correlation length $\bar{L}_0$ = 0.3, 1, and 3 and standard deviations of 0.066, 0.1, and 0.2 keeping the mean at 0.2, i.e. with coefficients of variation of 1/3, 1/2, and 1. A series of Monte Carlo analyses were carried out under the same excitation but with different realizations of the coefficients of friction and for each such analysis the power spectral density of the stationary response of the 5 oscillators was determined. A statistical analysis was then performed to obtain, for each frequency, the 5th and 95th percentiles of the power spectrum values which form the lower and upper boundaries of the "uncertainty band" on the response, see Figs 5 and 6. It appears from these figures and from results conducted at different excitation levels (not shown here for brevity) that the uncertainty bands are most affected by the level of variability of the coefficients of friction with the correlation length having only a small, localization type effect on the response of the oscillators closest to the wall.
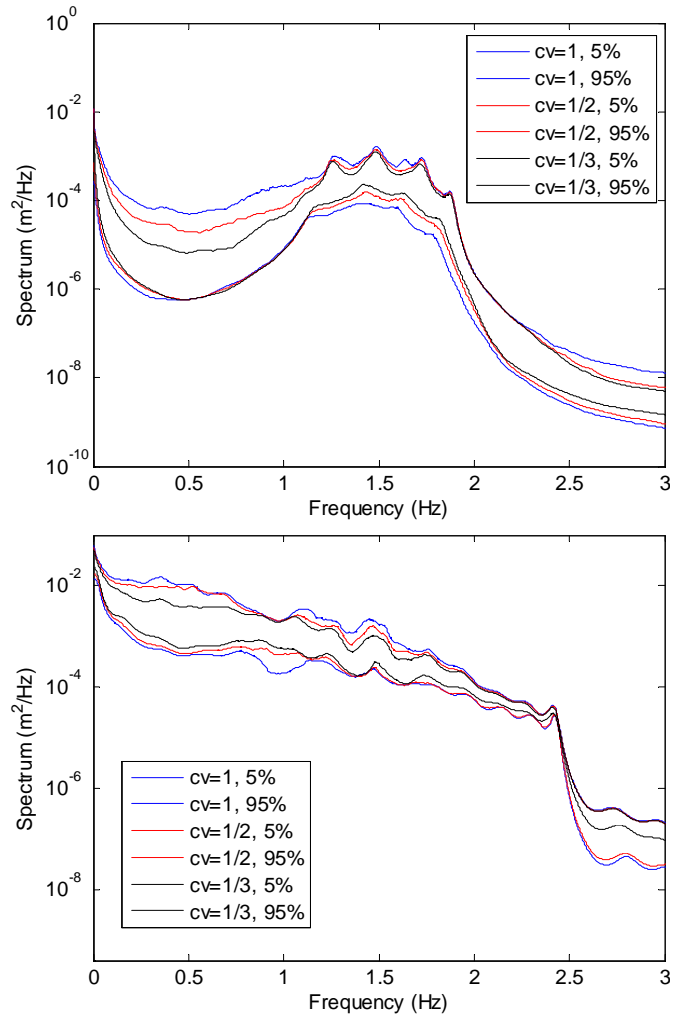

Figure 5. Uncertain bands on the power spectral density of the response of oscillators (a) 1 and (b) 5. Correlation length $\bar{L}_0$ = 0.3, various coefficients of variation.
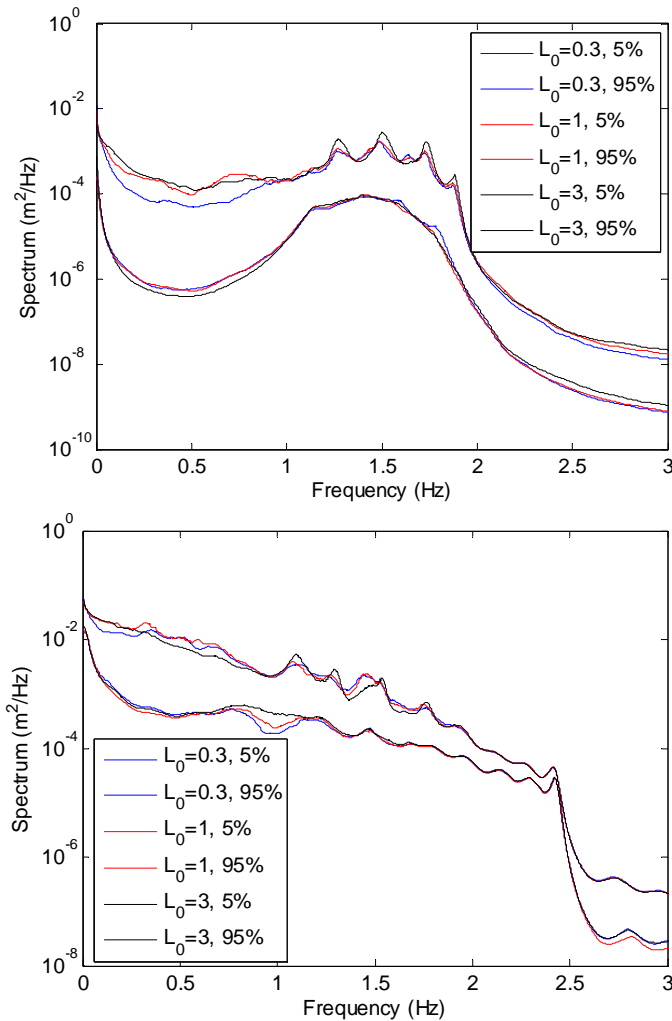
Figure 6. Uncertain bands on the power spectral density of the response of oscillators (a) 1 and (b) 5. Coefficients of variation of 0.3. Various correlation lengths $\overline{L}_0$.

4   SUMMARY

The focus of this investigation has been on the formulation and first assessment of a novel model for the representation of uncertain properties as discrete stationary random processes. As opposed to postulating the distribution of the random process values, this function is here derived to yield the maximum of the entropy under the set of constraints representing a given mean, a given variance, and a given correlation length. In the absence of a sign constraint on the process, its distribution is Gaussian with autocovariance function that is expressed in terms of the Lagrange multipliers of the constraints. A numerical approach was described and demonstrated for the evaluation of these Lagrange multipliers and the autocovariance functions found exhibit the features physically expected.

For positive processes, the distribution obtained is a truncated Gaussian and the above computational strategy was extended to allow the determination of the Lagrange multipliers and to efficiently simulate realizations of the process. Results obtained with different correlation lengths and coefficients of variation, up to a value of the latter of 1, suggest that the autocovariance function of the positive

process is very close to its equivalent for the process without sign constraint.

Next, the novel stochastic model of uncertainty proposed here was applied to the simulation of uncertain coefficients of friction. A chain of Iwan oscillators was considered to model the dynamic response of a flexible structure connecting through friction to a rigid foundation. Then, the response of this system subjected to a random load and with the uncertain coefficients of friction was analyzed by Monte Carlo simulations. The results of this computational effort confirm the sensitivity of the system response to uncertainty in the coefficients of friction and suggests that the correlation length of these coefficients plays a secondary role in the uncertainty on the response.

REFERENCES

[1]   R. Ghanem, and P.D. Spanos, Stochastic finite elements: a spectral approach, Spring-Verlag, New York, 1991.
[2]   M. Kleiber, D.H. Tran, T.D. Hien, 1992. The stochastic finite element method, John Wiley and Sons, New York, 1992.
[3]   G.I. Schueller (Ed.), A state-of-the-art report on computational stochastic mechanics, Probabilistic Engineering Mechanics, 12 (4) (1997) 197-321.
[4]   C. Soize, A nonparametric model of random uncertainties on reduced matrix model in structural dynamics, Probabilistic Engineering Mechanics, 15 (3) (2000) 277-294.
[5]   C. Soize, Maximum entropy approach for modeling random uncertainties in transient elastodynamics, Journal of the Acoustical Society of America, 109 (5) (2001) 1979-1996.
[6]   C. Soize, Non-Gaussian positive-definite matrix-valued random fields for elliptic stochastic partial differential operators, Computer Methods in Applied Mechanics and Engineering, 195 (2006), 26–64.
[7]   J.P. Den Hartog, Forced vibrations with combined coulomb and viscous friction. Transactions American Society of Mechanical Engineers. 9 (53) (1931) 107-115.
[8]   W.D. Iwan, Y, Zhang, Protecting base-isolated structures from near-field ground motion by turned interaction damper, Journal of Engineering Mechanics, 128 (3) (2002) 287-295.
[9]   A. Sinha, J.H., Griffin, Effects of friction dampers on aerodynamically unstable rotor stages, AIAA Journal, 23 (2) 262-270.
[10]   E.J. Berger, D.V. Deshmukh, Convergence behaviors of reduced-order models for friction contacts, Journal of Vibration and Acoustics, 127, (2005) 370-381.
[11]   D.V. Deshmukh, E.J. Berger, M.R. Begley, U. Komaragiri, Correlation of a discrete friction (Iwan) element and continuum approaches to predict interface sliding behavior, European Journal of Mechanics A/Solids 26 (2007) 212-224.